Power Quality Improvement with PV/Battery Hybrid Energy Conversion System Using HGICB DC-DC Converter

E. Rambabu[1], Snehalatha Penumalli[2], Mounika Irakamsetty[3], Susmitha Lanka[4], Venkata Sumanth Bogyam[5]

[1]Assistant Professor, Sree Venkateswara College of Engineering, North Rajupalem, Nellore, Andhra Pradesh, India

[2, 3, 4, 5]Department of Electrical Engineering, Sree Venkateswara College of Engineering, North Rajupalem, Nellore, Andhra Pradesh, India

Abstract: *The photovoltaic(PV)/battery hybrid energy conversion system is integrated with grid along with (i) multi functional features of micro grid side bidirectional voltage source converter(µG-VSC) ,(ii) tight voltage regulation capability of battery converter,(iii) MPPT tracking performance of high gain integrated cascaded boost converter which is having quadratic gain and less current ripples. In this paper the PV side converter is controlled by MPPT,P&O algorithm. This paper also proposes a modified instantaneous symmetrical component theory along with a PI controller to the µG-VSC in micro grid applications with following intelligent functionalities (a) to feed the generated active power in proportional to irradiation levels into the grid (b) compensation of the reactive power, (c) load balancing and (d) mitigation of current harmonics generated by non-linear loads, if any, at the point of common coupling (PCC), thus enabling the grid to supply only sinusoidal current at unity power factor. The battery energy storage system (BESS) is regulated to balance the power between PV generation and utility grid. A new control algorithm is also proposed in this paper for the battery converter with tight DC link voltage regulation capability. The dynamic performance of battery converter is investigated and compared with conventional average current mode control (ACMC). A model of a hybrid PV Energy Conversion System is developed and simulated in MATLAB/SIMULINK environment. The effectiveness of the proposed control strategies for HGICB converter and µG-VSC with battery energy conversion system are validated through extensive simulation studies.*

Keywords: HGICB, MPPT, P&O, Instantaneous symmetrical component Theory

1. Introduction

Due to the development of science and technology, power demand is increasing day-by-day. So to reach that particular demand we go for renewable energy resource [1]. There are many renewable resources like solar, wind, tidal etc.., among these renewable resources PV and Wind power are most rapidly growing renewable energy sources. As we know that this pv source is non-linear energy source it will not give optimum utilization of pv system when it is directly connected. So to utilize this pv source optimally we provide an intermediate electronic controller in between source and load under all operating conditions[2].By using this electronic controller it is possible to operate the pv source at maximum power point so that the energy efficiency of the pv system can also be increased. There are many control algorithms which is used to track the maximum power from the pv arrays, such as incremental conductance (INC),constant voltage(CV),and perturbation and observation(P&O).Incremental conductance and perturbation & observation are the two methods[2],[3]. Which are often used to achieve maximum power point tracking.

There are many DC-DC converter topologies are available to track the maximum power point in generating system. It provides wider conversion ratios [4] when the conventional converters are connected in cascade. One of the major advantages of this converter is a high gain and low current ripple. But, this configuration has also a drawback that the total efficiency may become low if the numbers of stages are high, owing to power losses in the switching devices [4] quadratic converter configuration is also available that uses

single switch and achieves quadratic gain [4]. An interesting attractive converter topology is a high gain integrated cascaded boost converter [4] this class of converters can be used only when the required number of stages is not very large, else the efficiency will be reduced. However, this class of converters for PV applications are not reported in the technical literature. Micro-grid power converters can be classified into (i) grid-feeding, (ii) grid-supporting, and (iii) grid-forming power converters [5]. There are many control schemes reported in the literature such as synchronous reference theory, power balance theory, and direct current vector control [6], [7], for control of µG-VSC in micro grid application.

2. System Description

The envisaged system consists of a PV/Battery hybrid system with the main grid connecting to non-linear and unbalanced loads at the PCC as shown in the Fig. 1. The photovoltaic is modeled as nonlinear voltage sources [8]. The PV array is connected to HGICB dc-dc converter and bidirectional battery converter are shown in Fig. 1, which are coupled at the dc side of a µG-VSC. The HGICB dc-dc converter is connected to the PV array works as MPPT controller and battery converter is used to regulate the power flow between dc and ac side of the system.

3. Modeling and Control

The MPPT algorithm for HGICB Converter, control approaches for battery converter and µG-VSC are discussed in the following sections.
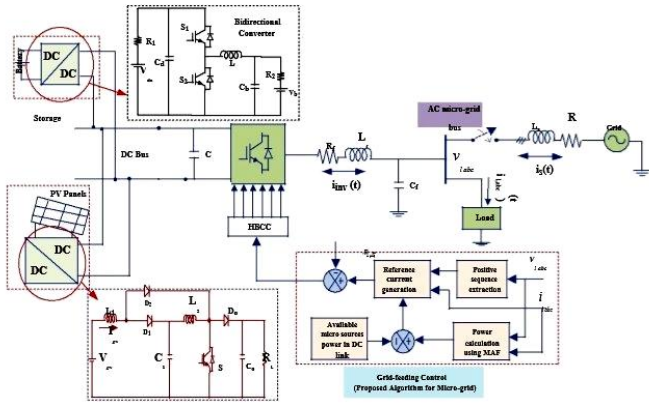
Figure 1: Block Diagram of Hybrid Energy conversion system under consideration

3.1 PV Array Model

Photo voltaic (PVs) are arrays (combination of cells) that contain a solar voltaic material which converts solar energy into electrical energy. PV cell is a basic device for Photovoltaic Systems. Such systems include multiple components like mechanical and electrical connections and mountings and various means of regulating and (if required) modifying the electrical output. Materials that are used for photovoltaic are mono crystalline silicon, polycrystalline silicon, microcrystalline silicon, cadmium telluride and copper indium selenide . The current and voltage available at the PV device terminals can be directly used to feed small loads like lighting systems or small DC motors. The output characteristics of PV module depends on the solar irradiance, the cell temperature and output voltage of PV module. Since PV module has nonlinear characteristics, it is necessary to model it for the design and simulation of maximum power point tracking (MPPT) for PV system applications.

3.2 Battery Converter Modeling

The battery converter goes through two topological stages in each switching period, its power stage dynamics can be described by a set of state equations. The average state space model of the converter can therefore be given as:

$$\frac{di_L}{dt} = \frac{v_{c1}d_{(t)}}{L} - \frac{v_{c2}}{L} - \frac{(r_s + r_L)i_L}{L}$$

$$\frac{dv_{c1}}{dt} = \frac{v_{dc,Bus} - v_{c1}}{c_1 R_1} - \frac{i_L d_{(t)}}{c_1} \quad \ldots\ldots\ldots (1)$$

$$\frac{dv_{c2}}{dt} = \frac{v_B - v_{c2}}{c_2 R_2} - \frac{i_L}{c_2}$$

The averaged model is nonlinear and time-invariant because of the duty cycle, d (t).

This model is finally linearized about the operating point to obtain a small-signal model is shown in Fig. 4. The following are the important transfer functions used to design the compensators and to analyze the system behavior under small signal conditions (i) the duty-cycle-to-output transfer function Gcv (s), carries the information needed to determine the type of the voltage feedback compensation,(ii) the duty-cycle-to-inductor current transfer function Gci(s), is needed to determine the current controller structure.
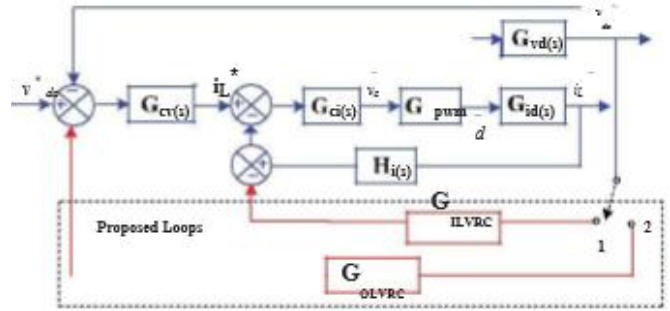

Figure 2: Inner and outer loops of battery converter with MACMC

3.3 Proposed Control for Battery Converter

If AC side of μG-VSC has constant power appliances (CPAs), in the small-signal sense, CPAs nature leads to negative incremental input-conductance which causes de-stabilization of the dc-link voltage [10]. On the micro-grid generation side, the inherent negative admittance dynamics of their controlled conversion stages challenges the dc-link voltage control and stability. This effect is more with reduced dc-link capacitance. Therefore, in both cases, fast and effective control and stabilization of the dc-link voltage is very crucial issue. To address this problem, many methods are reported in the literature like (i) by large DC link capacitance (ii) by adding passive resistances at various positions in DC LC filter (iii) by loop cancellation methods [9], [10].

In this paper, a new modified-ACMC (MACMC) control algorithm is proposed for effective control and stabilization of battery converter by introducing virtual resistance (VR) in the (i) outer loop called outer loop virtual resistance control (OLVRC) (ii) intermediate loop called inner loop virtual resistance control (ILVRC) as shown in Fig. 3. The proposed virtual resistance based dynamic damping methods aim at injecting a damping signal that compensate for negative conductance caused by CPAs without any power loss.
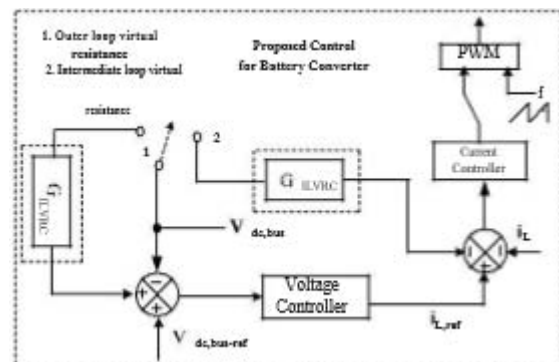

Figure 3: A new modified-ACMC control strategy for battery converter

3.4 Design steps for Compensators of BESS

The effectiveness of proposed VRCs control algorithm is investigated and compared with the use of traditional ACMC [11]. The flowchart for modes of operation of battery converter in grid feeding mode is shown in Fig. 3. The design guidelines for inner and outer loop compensators of ACMC

are given below. The inner loop (current) gain can be written as**:**

The inner loop (current) gain can be written as:
$$T_i(s) = G_i d_{(s)} R_i G_{ci}(s) F_m \qquad \ldots\ldots(2)$$
The outer loop (voltage) gain can be written as:
$$T_v(s) = G_v(s) G_{cs}(s)(1 + G_{ci}(s)) F_m \qquad \ldots\ldots(3)$$
and the overall loop gain therefore can be written as:
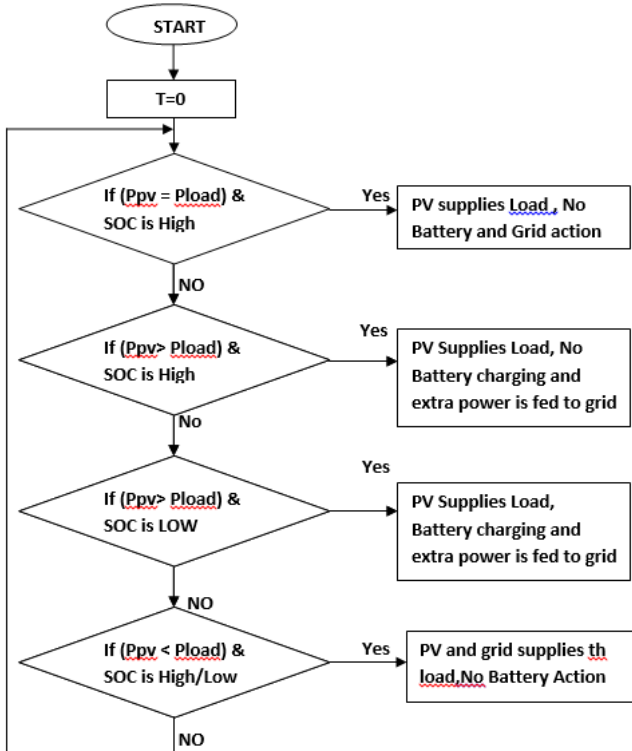$$T_1(s) = T_s + T_v \qquad \ldots\ldots\ldots(4)$$

Figure 4: Flow chart of power flow in hybrid system

Voltage loop design steps
i) Place one zero as high as possible, yet not exceeding resonating frequency of the converter.
ii) Place one pole at frequency of output capacitor ESR to cancel the effects of output capacitor ESR.
iii) Adjust, gain of compensator to trade-off stability margins and closed-loop performance.
iv) Another pole should be place at origin to boost the dc and low frequency gain of the voltage loop.

Similar steps mentioned above are followed to design current loop and for design of MACMC loops. Following the design procedure given above, the inner current and outer voltage loop compensators are designed to regulate the DC link voltage to 920 V.

3.5 Generation of reference currents for μG-VSC

The main aim of the μG-VSC control is to cancel the effects of unbalanced and harmonic components of the local load, while supplying pre-specified amount of real and reactive powers to the load. Upon successfully meeting this objective, the grid current i_g will then be balanced and so will be the PCC voltage v_p provided, grid voltage v_g is balanced. Let us denote the three phases by the subscripts a, b and c. Since i_g is balanced, we can write:

$$i_{ga} + i_{gb} + i_{gc} = 0 \ldots\ldots\ldots\ldots(5)$$
From the Figure 1, Kirchhoff's current law (KCL) at PCC gives
$$i_{g,abc} + i_{inv,abc} = i_{L,abc} \ldots\ldots\ldots\ldots\ldots(6)$$
Therefore, from (3.9) and (3.10), we can write as:
$$i_{inv,a} + i_{inv,b} + i_{inv,c} = i_{L,a} + i_{L,b} + i_{L,c} \ldots\ldots(7)$$
Since i_g is balanced due to the action of the compensator, the voltage v_p will also become balanced. Hence, the instantaneous real powers Pg will be equal to its average component. Therefore, we can write
$$P_g = v_{pa} i_{ga} + v_{pb} i_{gb} + v_{pc} i_{gc} \qquad \ldots\ldots\ldots(8)$$

Table 1: System Parameter

System Quantities	Values
System voltages	325 V peak phase to neutral, 50 Hz
Linear Load	Zla = 50 + j1.57 Ω, Zlb = 45 + j3.14 Ω, Zlc = 40 + j4.71 Ω
Non-Linear Load	Three phase full bridge rectifier load feeding a R-L load of 44Ω-3 mH
G-VSC parameters	Cdc=660 μF,Vdcref =920 V, Lf = 5 mH, Rf = 0.1Ω
Hysteresis band	0.25A

solving above equations, the μG-VSC reference currents are obtained as follows

$$i^*_{inv,a} = i_{la} - \frac{v_{ga} + \beta(v_{gb} - v_{gc})}{\Delta}(P_{lavg} - P_{\mu s} + P_{loss})$$

$$i^*_{inv,b} = i_{lb} - \frac{v_{gb} + \beta(v_{gc} - v_{ga})}{\Delta}(P_{lavg} - P_{\mu s} + P_{loss})$$

$$\ldots\ldots(9)$$

Where, $\Delta = \sum_{j=a,b,c} v_{gj}^2, \beta = \tan\frac{\phi}{\sqrt{3}} = \frac{Q_s}{P_s\sqrt{3}}$

and, $Q_s = Q_l - Q_{\mu s}$ and by substituting $\beta P_s = \frac{Q_s}{\sqrt{3}}$ into the equation(9), the modified G-VSC reference current equations in terms of active and reactive components are obtained as:

$$i^*_{inv,a} = i_{la} - \frac{v_{ga} P_s}{\sum_{j=a,b,c} v_{gj}^2} - \frac{(v_{gb} - v_{gc})Q_s}{\sum_{j=a,b,c} v_{gj}^2 \sqrt{3}}$$

$$i^*_{inv,b} = i_{lb} - \frac{v_{gb} P_s}{\sum_{j=a,b,c} v_{gj}^2} - \frac{(v_{gc} - v_{ga})Q_s}{\sum_{j=a,b,c} v_{gj}^2 \sqrt{3}}$$

$$i^*_{inv,c} = i_{lc} - \frac{v_{gc} P_s}{\sum_{j=a,b,c} v_{gj}^2} - \frac{(v_{ga} - v_{gb})Q_s}{\sum_{j=a,b,c} v_{gj}^2 \sqrt{3}} \qquad \ldots\ldots(10)$$

In equations (9) and (10), $P_{\mu s}$, P_{lavg}, and Q_l are the available micro source power, average load power, and load reactive power respectively. Ploss denotes the switching losses and ohmic losses in actual compensator. The term P_{lavg} is obtained using a moving average filter of one cycle window of time T in seconds.

4. Simulation Results

The proposed control strategies for PV hybrid generating system is developed and simulated using Matlab/SIMULINK under different solar insolation levels. In order to capture the transient response of the proposed control system, PV insolation is assumed to increase from 200 to 1000 W/m^2 at 0.3 s, and decreases from 1000 to 200 W/m^2 at 0.5 s.

This abrupt increase or decrease is assumed in this work in order to test the robustness of the proposed control algorithm. As a result, the inductor current of the HGICB converter is varied to track the maximum power accordingly and the power flow Between the µG-VSC, grid and load is also varied under above the operating conditions.

Table 2: Maximum Power Point Tracking Performance

Time(s)	G (W/m^2)	Vpv$_{ref}$(V)	Ipv$_{ref}$ (A)	Ppv$_{max}$ (KW)
0.2-0.3	200	190	14	2.5
0.3-0.5	1000	142	87	12.5
0.5-1	200	190	14	2.5

a) MPPT Tracking Performance of HGICB Converter

The dynamic performance of HGICB converter with P&O, MPPT algorithm at two different insolation levels are shown in Fig. 5. A variable PV voltage and current in proportion to insolation levels are applied to HGICB converter and as a result, the duty cycle is calculated using the MPPT algorithm. The PV characteristics at two insolation levels are shown in Fig. 5(a)-(b). From Fig. 5 (a), the maximum power, current and voltage are 2.6 kW, 14 A and 190 V respectively and these values are tracked by HGICB converter which are shown in Fig. 5 (d)-(f). Tracked values of PV power, voltage and currents are given in Table II for the above operating insolation levels. From these results it can be concluded that, HGICB converter is tracking maximum power closely at all operating conditions.
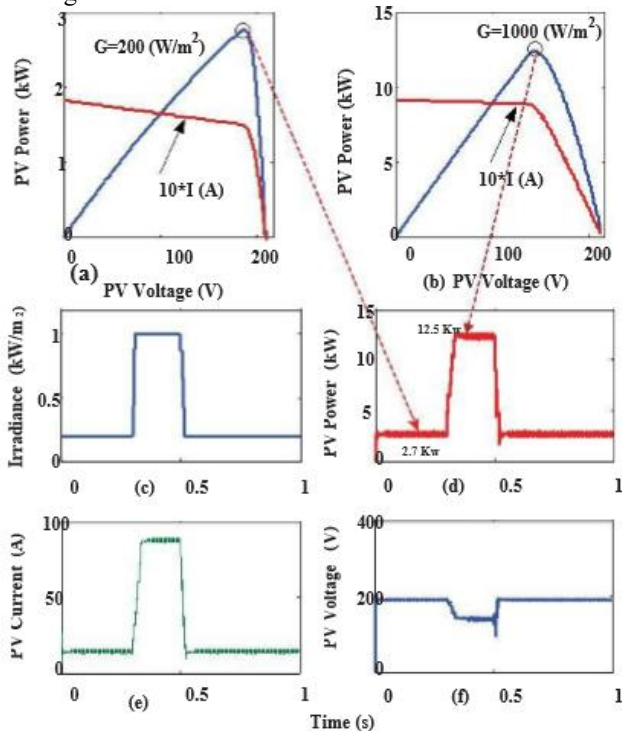

Figure 5: Simulation results: MPPT Tracking performance of HGICB Converter (a) PV Characteristic at G=200 W/m 2 (b) PV Characteristic at G=1000 W/m 2 (c) insolation variations (d) PV Maximum Power (e) PV Current (f) PV Voltage

b) Performance Of µG-VSC with Different Insolations

The µG-VSC is actively controlled to inject the generated active power as well as to compensate the harmonic and reactive power demanded by the unbalanced and non-linear load at PCC, such that the current drawn from grid is purely sinusoidal at UPF. The dynamic compensation performance of µG-VSC using proposed control algorithm with insolation change and non linear unbalanced load currents are shown in the Fig. 6 (a)-(d) along with grid side currents. When insolation G = 200 W/m^2, the maximum power extracted from PV arrays is 2.5 kW and the total dc load power (4.5 kW) is partly supplied by PV arrays and the remaining dc load power (2 kW) is drawn from grid through the bidirectional µG-VSC. Here observed that the power flows from ac side to dc link as shown in the Fig. 7. When insolation G = 1000 W/m 2 , the maximum power available from PV arrays is 12.5 kW, part of this power (4.5 kW) is supplied to dc load and remaining power (8 kW) is supplied to the ac load through bidirectional µG-VSC. In this case, the power flows from dc link to ac side. This shows the bidirectional power flow capability of µG-VSC. These dynamics of power flows can be seen from Fig. 7. The corresponding variations in the grid current against grid voltage with UPF are shown in the Fig.   along with dc link voltage
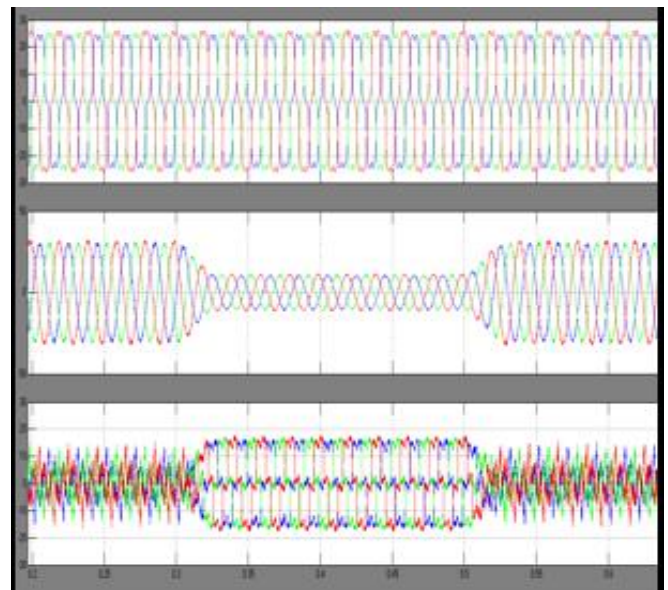

Figure 6: Simulation results using proposed control approach for Micro-grid side VSC: (a) Insolation Changes (b) Load currents (c) Grid currents (d) µG-VSC currents.
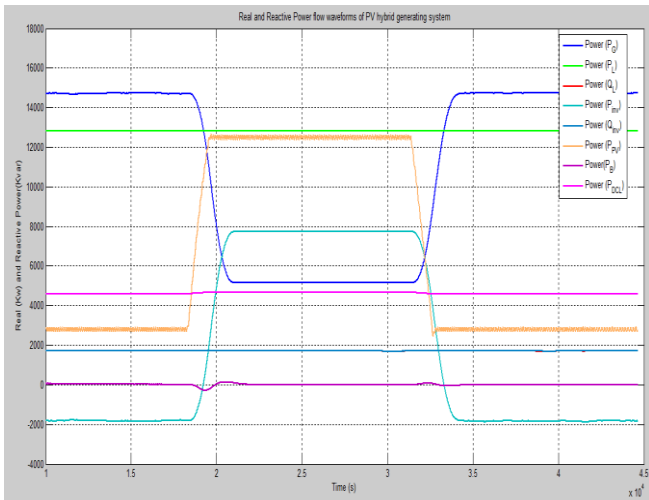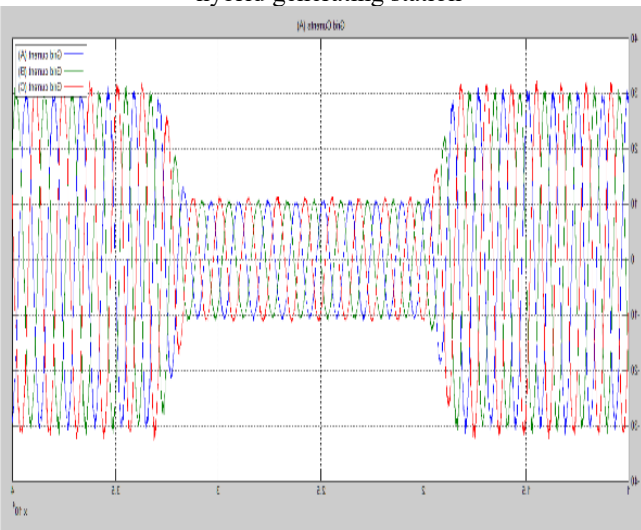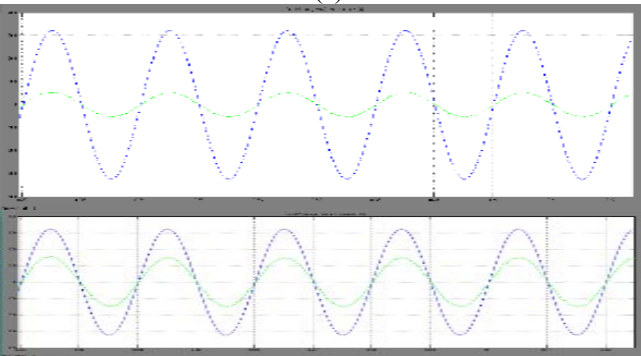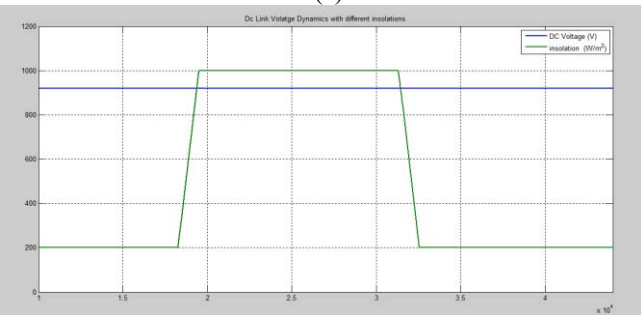
Figure 7: Real and reactive power flow waveforms of PV hybrid generating station

(a)

(a)

(b)

Figure 8: Simulation results: performance of proposed control approach (a)Grid Voltages and currents (b)DC link Voltage Dynamics with Different insolations.
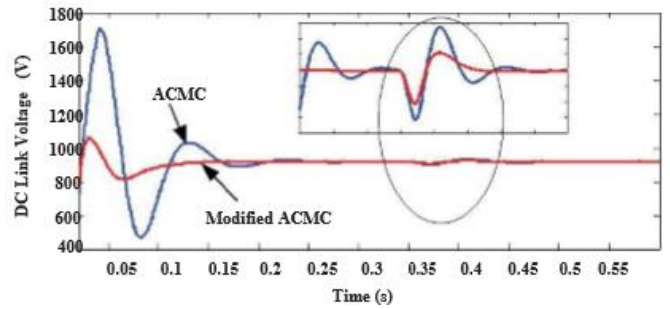

Figure 9: Dc Link Voltage Dynamics Using ACMC And MACMC Control Algorithms

5. Conclusion

The performance of PV/Battery hybrid energy conversion system has been demonstrated with the application of modified instantaneous symmetrical components theroy to µG-VSC proposed in this paper, an efficient control strategy is also proposed for battery converter to regulate the dc bus voltage tightly, under varying solar insolation and dc load conditions. HGICB converter topology is used to track the MPPT with high gain and less current ripple. The µG-VSC is able to inject the generated power into the grid alongwith harmonic and reactive power compensation for unbalanced non-linear load at the PCC simultaneously. The system works satisfactorily under dynamic conditions. The simulation results under a unbalanced non-linear load with current THD of 12% confirm that the µG-VSC can effectively inject the generated active power along with power quality improvement features and thus, it maintains a sinusoidal and UPF current at the grid side with THD of 1.68%
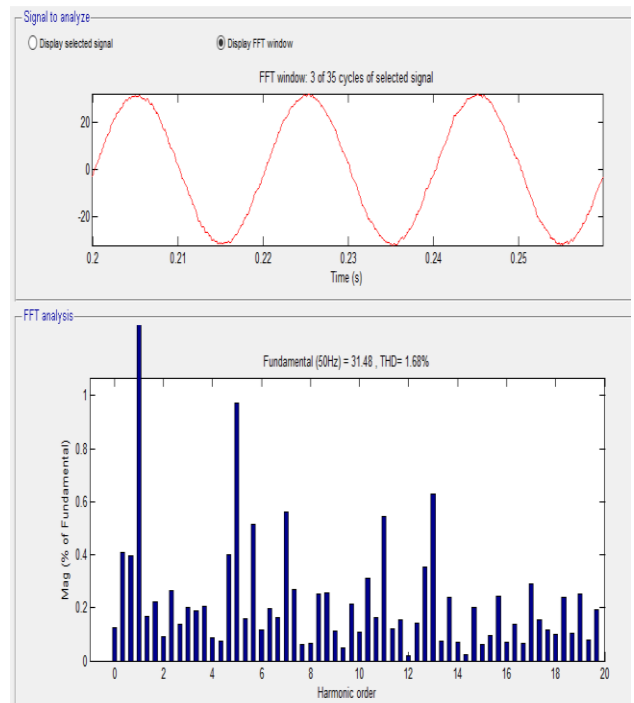

Figure 11: THD Value

References

[1] J. Carrasco, L. Franquelo, J. Bialasiewicz, E. Galvan, R. Guisado, M. Prats, J. Leon, and N.

Moreno-Alfonso, ―Power-electronic systems for the grid integration of renewable energy sources: A survey,‖ IEEE Trans. Ind. Electron., vol. 53, no. 4, pp. 1002 – 1016, Jun. 2006.

[2] M. de Brito, L. Galotto, L. Sampaio, G. de Azevedo e Melo, and C. Canesin, ―Evaluation of the main mppt techniques for photovoltaic applications,‖ IEEE Trans. Ind. Electron., vol. 60, no. 3, pp. 1156 – 1167, Mar. 2013.

[3] B. Subudhi and R. Pradhan, ―A comparative study on maximum power point tracking techniques for photovoltaic power systems,‖ IEEE Trans. Sustain. Energy, vol. PP, no. 99, pp. 1 –10, Mar. 2012.

[4] W. Li and X. He, ―Review of nonisolated high-step-up dc/dc converters in photovoltaic grid-connected applications,‖ IEEE Trans. Ind. Electron., vol. 58, no. 4, pp. 1239 –1250, Apr. 2011.

[5] J. Rocabert, A. Luna, F. Blaabjerg, and P. Rodri andguez, ―Control of power converters in ac microgrids,‖ IEEE Trans. Power Electron., vol. 27, no. 11, pp. 4734 –4749, Nov. 2012.

[6] R. Kadri, J.-P. Gaubert, and G. Champenois, ―An improved maximum power point tracking for photovoltaic grid-connected inverter based on voltage-oriented control,‖ IEEE Trans. Ind. Electron., vol. 58, no. 1, pp. 66 –75, Jan. 2011.

[7] S. Zhang, K.-J. Tseng, D. Vilathgamuwa, T. Nguyen, and X.-Y. Wang, ―Design of a robust grid interface system for pmsg-based wind turbine generators,‖ IEEE Trans. Ind. Electron., vol. 58, no. 1, pp. 316–328, Jan. 2011.

[8] A. Chatterjee, A. Keyhani, and D. Kapoor, ―Identification of photovoltaic source models,‖ IEEE Trans. Energy Convers., vol. 26, no. 3, pp. 883 –889, Sept. 2011.

[9] A. Rahimi, G. Williamson, and A. Emadi, ―Loop-cancellation technique: A novel nonlinear feedback to overcome the destabilizing effect of constant-power loads,‖ IEEE Trans. Veh. Technol., vol. 59, no. 2, pp. 650 –661, Feb. 2010.

[10] A. Radwan and Y. Mohamed, ―Modeling, analysis, and stabilization of converter-fed ac microgrids with high penetration of converter- interfaced loads,‖ IEEE Trans. Smart Grid., vol. 3, no. 3, pp. 1213 – 1225, Sept. 2012.

[11] W. Tang, F. Lee, and R. Ridley, ―Small-signal modeling of average current- mode control,‖ IEEE Trans. Power Electron., vol. 8, no. 2, pp. 112 –119, Apr. 1993.

Author Profile

P.Snehalatha pursuing B.Tech in Sree Venkateswara College of Engineering, Nellore, JNTU Anantapur. Andhra Pradesh

I. Mounika pursuing B.Tech in Sree venkateswara college of engineering, Nellore, JNTU Anantapur, Andhra Pradesh

B. Venkata Sumanth pursuing B.Tech in Sree venkateswara college of engineering, Nellore, JNTU Anantapur, Andhra Pradesh

L.Susmitha pursuing B.Tech in Sree Venkateswara College of engineering, Nellore, JNTU Anantapur, Andhra Pradesh

E. Rambabu obtained his B. Tech degree in Electrical and Electronics Engineering from VRS&YRN College of Engineering.. He obtained his M. Tech degree in Power Electronics and Electric Drives, Mother Theresa Institute of Science & Technology. Sathupalli. Currently, he is working as Assistant Professor in Sree Venkateswara College of Engineering, Nellore. .